THE JOURNAL OF BIOLOGICAL CHEMISTRY VOL. 286, NO. 10, pp. 8128–8140, March 11, 2011

Homology-based Identification of Capsid Determinants That Protect HIV1 from Human TRIM5α Restriction*[S]

Received for publication, September 22, 2010, and in revised form, December 15, 2010 Published, JBC Papers in Press, December 17, 2010, DOI 10.1074/jbc.M110.187609

Pierre V. Maillard[‡], Vincent Zoete[§], Olivier Michielin[§¶‖], and Didier Trono[‡1]

From the [‡]Global Health Institute, School of Life Sciences, and "Frontiers in Genetics" National Center for Competence in Research, Ecole Polytechnique Fédérale de Lausanne and the [§]Swiss Institute of Bioinformatics, Molecular Modeling Group, Genopode Building, 1015 Lausanne, Switzerland, the [¶]Ludwig Institute for Cancer Research, Ltd., 1066 Epalinges, Switzerland, and the [‖]Pluridisciplinary Centre for Clinical Oncology (CePO), Lausanne University Hospital (CHUV), 1011 Lausanne, Switzerland

The tropism of retroviruses relies on their ability to exploit cellular factors for their replication as well as to avoid host-encoded inhibitory activities such as TRIM5α. N-tropic murine leukemia virus is sensitive to human TRIM5α (huTRIM5α) restriction, whereas human immunodeficiency virus type 1 (HIV1) escapes this antiviral factor. We previously revealed that mutation of four critical amino acid residues within the capsid can render murine leukemia virus resistant to huTRIM5α. Here, we exploit the high degree of conservation in the tertiary structure of retroviral capsids to map the corresponding positions on the HIV1 capsid. We then demonstrated that, when changes were introduced at some of these positions, HIV1 becomes sensitive to huTRIM5α restriction, a phenomenon reinforced by additionally mutating the nearby cyclophilin A binding loop of the viral protein. These results indicate that retroviruses have evolved similar mechanisms to escape TRIM5α restriction via the interference of structurally homologous determinants in the viral capsid.

Viruses are obligatory parasites that require specific components of the host cell machinery to replicate. However, their tropism also depends on their ability to overcome host-encoded intracellular antiviral activities termed restriction factors (1, 2). TRIM5α is one such activity that restricts retroviruses by targeting their capsid early after viral entry, thus provoking the premature uncoating of incoming virions (3–5).

TRIM5α is part of the tripartite motif (TRIM)[2] protein family, characterized by the presence of a RING finger, a B-Box II, and a coiled-coil domain collectively forming the so-called RBCC motif (6, 7). TRIM5α also contains a C-terminal PRYSPRY domain responsible for direct binding to the retroviral capsid (CA) (8–12). Species-specific amino acid variations, notably in the PRYSPRY domain, dictate the spectrum of retroviruses restricted by different TRIM5α orthologues (13–15). Remarkably, a given TRIM5α species can target a wide range of retroviruses. For example, human TRIM5α (huTRIM5α) blocks gammaretroviruses such as N-tropic murine leukemia virus (N-MLV) as well as lentiviruses such as feline immunodeficiency virus (FIV) and equine infectious anemia virus, but it cannot efficiently block human immunodeficiency viruses types 1 (HIV1) and 2 (HIV2) (16–20). In contrast, rhesus macaque TRIM5α (rhTRIM5α) can inhibit all of theses viruses albeit with variable efficiencies (21, 22).

The retroviral capsid is derived from the proteolytic cleavage of the Gag (group-specific antigen) precursor, which provides all the structural elements responsible for organizing the virion (23). Gag is synthesized as a polyprotein of 55 kDa that assembles at the plasma membrane together with the viral genome, leading to the release of immature virions. Gag is then cleaved by the viral protease to generate matrix, CA, and nucleocapsid homomultimers that reassemble to form the three inner shells of the mature virion. Although matrix lies beneath the envelope-bearing viral outer lipid bilayer, CA forms the virion inner core, wrapping the nucleocapsid-associated viral genome and enzymes (23).

Mature retroviral capsids can adopt spherical (*e.g.* MLV), cylindrical (*e.g.* Mason-Pfizer Monkey virus) or conical (*e.g.* HIV) morphologies, but despite these differences, they exhibit a remarkable degree of structural conservation, all deriving from a hexagonal array of hexameric CA monomers (24–28). Assembly is stabilized by homophilic interactions between the N- and C-terminal CA domains. The C-terminal domain, which is buried inside the capsid, mediates both interhexameric and intrahexameric contacts, whereas the N-terminal domain (NTD), exposed at the surface, forms the hexameric rings. Remarkably, although CA proteins from different retroviruses display little sequence identity, their tertiary structures are highly conserved (27, 29–38). The NTD is composed of six (MLV) or seven (HIV) α-helices, and for lentiviruses only, it includes an extended loop between helix 4 and 5. In the case of HIV1 and FIV, this loop is known to bind the cellular peptidyl prolyl *cis-trans* isomerase cyclophilin A (CypA) (32, 39–41).

* This work was supported by the Swiss National Science Foundation, the Infectigen Association, and the Strauss Foundation.

[S] The on-line version of this article (available at http://www.jbc.org) contains supplemental Tables S1 and S2 and Fig. S1.

[1] To whom correspondence should be addressed: EPFL SV GHI LVG, SV 3805 (Bâtiment SV), Station 19, CH-1015 Lausanne, Switzerland. Tel.: 41-21-693-17.51; E-mail: didier.trono@epfl.ch.

[2] The abbreviations used are: TRIM, tripartite motif; huTRIM5α, human TRIM5α; rhTRIM5α, rhesus TRIM5α; sqTRIM5α, squirrel TRIM5α; MLV, murine leukemia virus; Mo-MLV, Moloney MLV; N-MLV, N-tropic MLV; B-MLV, B-tropic MLV; HIV, human immunodeficiency virus; HIV1, HIV type 1; HIV2, HIV type 2; FIV, feline immunodeficiency virus; NTD, N-terminal domain; SIV, simian immunodeficiency virus; SIVagm, SIV from African green monkey; SIVmac, SIV from macaque; CsA, cyclosporine; MDTF, *M. dunni* tail fibroblast; CA, capsid; CypA, cyclophilin A; Gag, group-specific antigen.

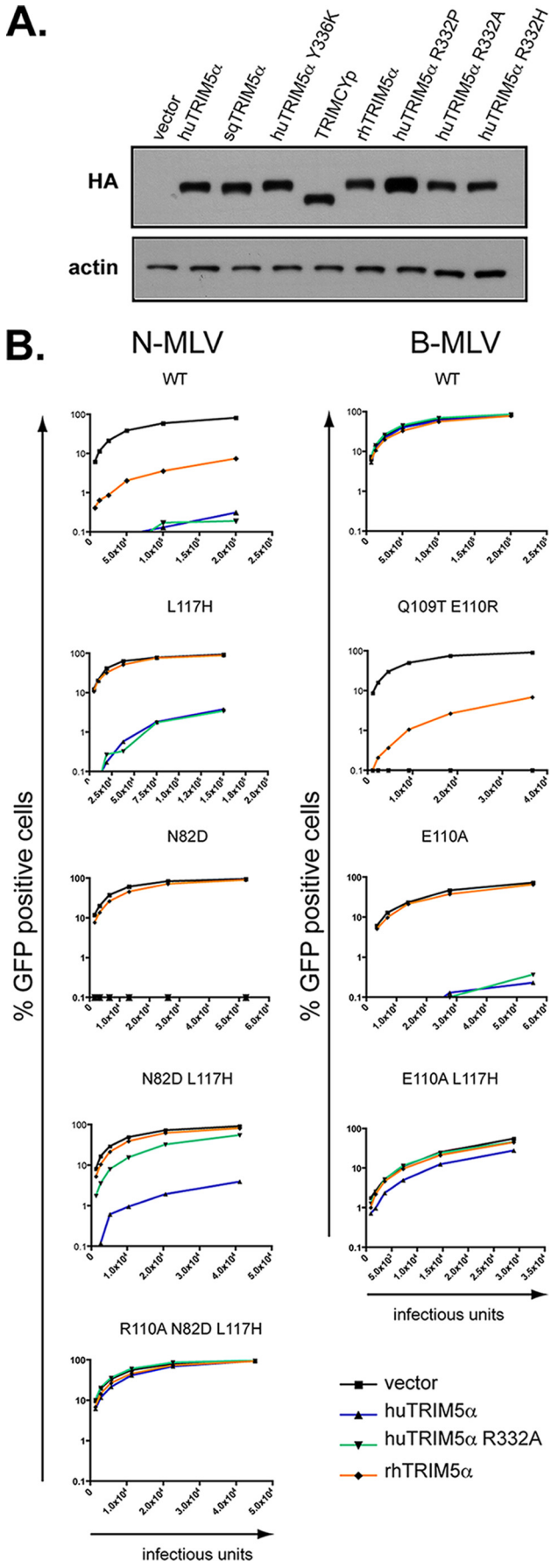

The precise role of CypA during HIV1 infection is still not well understood, yet many studies suggest that it facilitates viral disassembly (39, 42–46). CypA is packaged into the virions during viral assembly through binding with the CA moiety of the Gag polyprotein (47–49). CypA is recruited by CA proteins from HIV1, FIV, simian immunodeficiency virus (SIV) from African green monkeys (SIVagm) and chimpanzee but not from other lentiviruses such as equine infectious anemia virus and SIV from macaque (SIVmac) (41, 47–52).

The CA-CypA interaction can be prevented by mutating CA at positions 89 (CA89) and 90 (CA90) or by using the competitive inhibitor cyclosporine A (CsA). This leads to a decrease in HIV1 infectivity in human cells through mechanisms that are still unclear (44, 47, 49). Although CypA can both bind to and catalyze the *cis-trans* isomerization of the peptide bond between HIV1 CA89 and CA90, it is not known which of these two properties is required for its effect on viral infectivity (42). However, CsA-based experiments have revealed that CypA recruitment in target rather than producer cells is responsible for boosting HIV1 infectivity (53).

CypA has also been demonstrated to impact upon TRIM5α-mediated restriction. In particular, HIV-1 restriction by TRIM5α from Old World monkeys such as rhesus macaque is impaired when target cells are treated with CsA or CypA-directed RNA interference or, to some extent, by mutating the cyclophilin binding loop of CA (54–56). In contrast, the positive effect of CypA on HIV1 replication in human cells is independent of TRIM5α (55, 57). Remarkably, retrotransposition of the CypA coding sequence into the *TRIM5* gene has occurred on two independent occasions during primate evolution (58–64). As a result, owl monkeys (part of the New World monkeys) as well as two macaque species (part of the Old World monkeys) express a chimeric protein, TRIMCyp, in which the PRYSPRY domain is replaced by CypA, allowing the capture of incoming retroviral capsids through a CypA-CA interaction. HIV1 successfully infects human cells partly due to its ability to escape huTRIM5α, a feat that N-MLV cannot accomplish. However, if the N-MLV capsid is mutated at four key positions (CA82, CA109, CA110, and CA117) situated at the edge of a cavity formed by helices 4–6, it is no longer inhibited by huTRIM5α (19, 65, 66).

Here, we take advantage of the high conservation of retroviral capsids to identify the corresponding positions of the HIV1 CA. Through a combination of genetic and functional studies, we then demonstrate that these positions can be engi-

FIGURE 1. **MLV capsid positions CA82, CA109, CA110, and CA117 influence restriction mediated by TRIM5α variants that have distinct retroviral specificities.** *A*, Western blot analysis of extracts from MDTF cells stably transduced with retroviral vectors expressing HA-tagged versions of the indicated TRIM5α variants using HA (*top*)- and actin (*bottom*)-specific antibodies is shown. All TRIM5α variants exhibited wild type levels of expression, except for huTRIM5α R332P, that was detected at slightly higher steady-state levels. *B*, MDTF cells expressing wild type (WT) or the indicated mutant forms of huTRIM5α or transduced with a control vector were challenged with serial 2-fold dilutions of MLV-based vectors harboring either a WT or the indicated mutated capsid. Infections were scored at 72 h post-infection by FACS. These results are representative of two independent experiments.

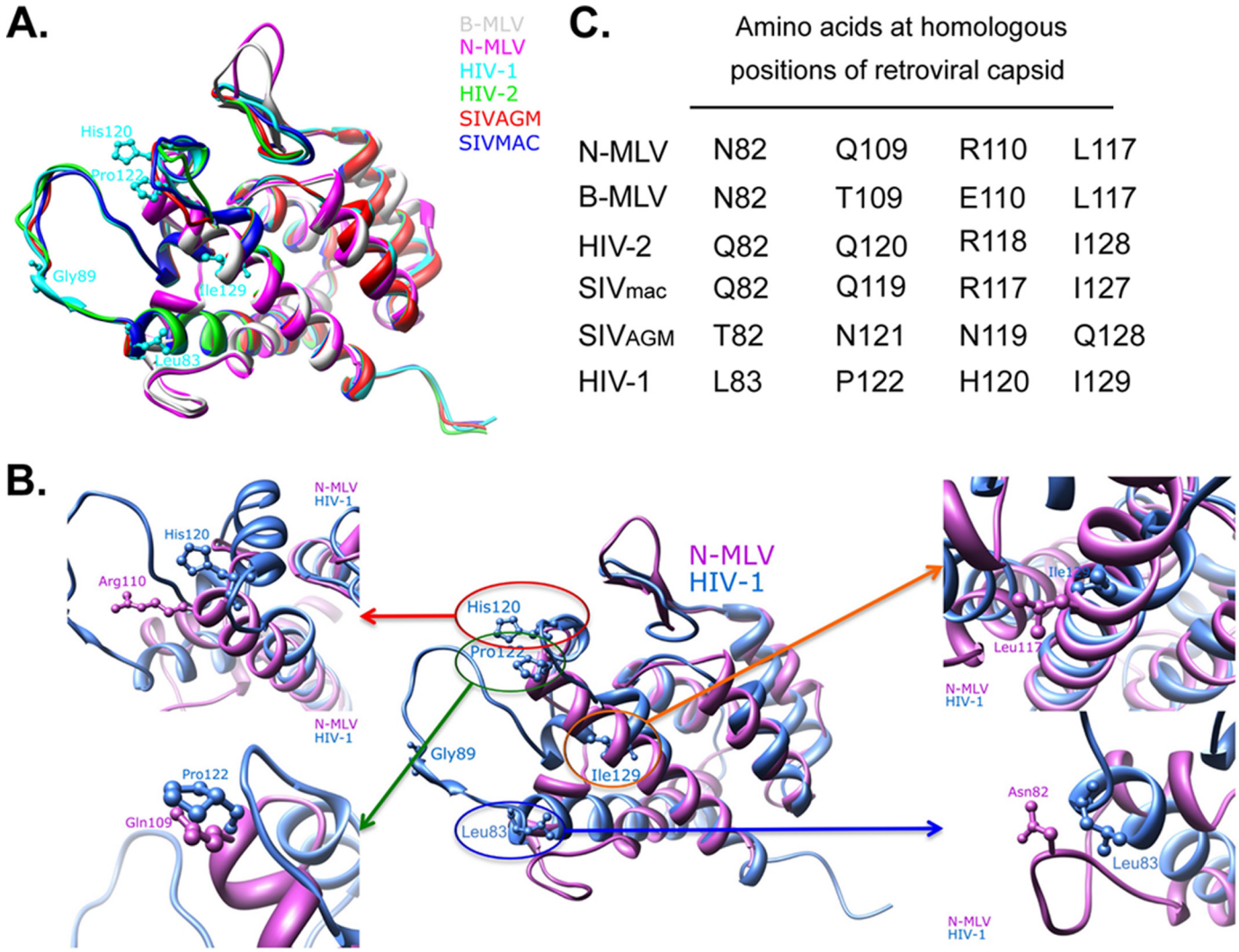

FIGURE 2. **Identification of positions on the HIV1 capsid that are structurally homologous to MLV CA82, CA109, CA110, and CA117.** *A*, shown is structural sequence alignment using known (HIV1 and N-and B-MLV) and predicted (HIV-2, SIVmac, and SIVagm) structures of retroviral capsid N-terminal domains (CA NTD) based on a combination of residue identity/similarity and secondary structure correspondence. Residues at the four positions on the HIV1 capsid (CA83, CA120, CA122, and CA129) homologous to MLV CA82, CA109, CA110, and CA117 are depicted in the superimposition CA NTDs. The glycine at HIV1 CA89 on the cyclophilin binding loop is also illustrated. Distinct colors are used to represent individual CA NTDs structures. *B*, the same structural sequence alignment as in *A* is shown but depicting only the N-MLV (*violet*) and HIV1 (*blue*) CA NTD (*central panel*) with the four HIV1 residues CA83, CA120, CA122, and CA129 shown. Highlighting these four positions shows the proximity and similar orientation of HIV1 CA120 with MLV CA110 (*top left*), HIV1 CA122 with MLV CA109 (*bottom left*), HIV1 CA129 with MLV CA117 (*top right*), and HIV1 CA83 with MLV CA82 (*bottom right*). *C*, shown are residues present at the four homologous positions from MLV in N- and B-MLV, HIV1, HIV2, SIVmac, and SIVagm. Of note, the previously unknown structure of the N-terminal domain of the HIV2 capsid has recently been resolved, whereas this present study was ongoing (64). Superimposition of the predicted model of the HIV2 capsid with its defined structure showed a low averaged root mean square deviation (0.9 Å) (supplemental Fig. S1).

neered to render HIV1 susceptible to huTRIM5α. We further reveal that this effect is amplified by preventing CA-CypA binding. Together, these results shed interesting light on the mechanisms of TRIM5α-mediated restriction and escape there from and highlight structural determinants of the virus that could serve as attractive drug targets.

EXPERIMENTAL PROCEDURES

Cell Lines and Culture—*Mus dunni* tail fibroblasts (MDTF) were purchased from the American Type Culture Collection and cultured in Dulbecco's modified Eagle's medium as described (66).

Plasmids—MLV-based particles were produced using packaging constructs N and B-tropic MLV (pCIG3-N and pCIG3-B) and the GFP-encoding construct pCNCG as described (66). HIV1-based vectors were produced with the packaging construct pCMVΔR8.74 and the vector pRRLsin PGK GFP. The *env* construct for all viral productions was pMD2G, expressing vesicular stomatitis virus G protein. The MLV plasmids encoding human, rhesus macaque TRIM5α, or owl monkey TRIMCyp (pLPCX-huTRIM5α-HA, pLPCX-rhTRIM5α-HA, pLPCX-TRIMcyp-HA) were kind gifts from J. Sodroski. The squirrel monkey TRIM5α sequence was amplified from pCXCR-sqTRIM5α (kindly provided by G. Towers) and fused in 3′ by PCR with the sequence encoding the influenza virus hemagglutinin (HA). The PCR product was inserted downstream of the CMV promoter of the MLV vector construct pLPCX (Clontech) allowing for puromycin selection of transduced cells. HuTRIM5α and MLV capsid mutants were already de-

scribed (66). All HIV1 capsid mutants were generated by site-directed mutagenesis of pCMVΔR8.74 using the XL QuickChange mutagenesis kit (Stratagene). All primers used in this study are listed in supplemental Table S2.

Homology Modeling and Structural Sequence Alignment of Retroviral Capsid Proteins—The HIV2 (Uniprot entry P04584 (67)), SIVagm (UniProt entry Q02836), and SIVmac (UniProt entry P05897) capsid protein sequences were defined as target sequences for homology modeling. Experimental crystal structures of HIV1 (PDB (68) ID 1AFV (37)), N-MLV (PDB ID 1U7K (27)), and B-MLV (PDB ID 3BP9 (38)) were used as structural templates. Multiple sequence alignment of the target and template sequences was performed using the MUSCLE algorithm (69, 70). HIV and SIV belong to the lentivirus retroviral genus (71), and the sequence identity between their capsid proteins ranges from 60 to 86%. MLV belongs to the gammaretroviral genus (71), and the sequence identity between the N-MLV and B-MLV capsid proteins is 97%. The sequence identity for the capsid proteins between the lentiviruses and gammaretroviruses is only around 13%. Based on the target-template sequence alignments, model structures of HIV-2, SIVagm, and SIVmac capsid proteins were built by satisfaction of spatial restraints using the MODELLER program Version 9.1 (72). 2000 models were built for each protein, and the final model was selected based on the modeler objective function.

The structural sequence alignments were performed using the MatchMaker command of the UCSF Chimera program (73). This alignment is based on a combination of residue identity/similarity and secondary structure correspondence. The former is obtained using the Needleman-Wunsch algorithm (74) with the BLOSUM-62 (75) residue similarity matrix, whereas the secondary structure assignment is computed with the Kabsch and Sander algorithm (76). The weights applied to the residue similarity and secondary structure during the computation of the structural alignments were 0.7 and 0.3, respectively.

Vector Production and Determination of Titers—HIV1-based GFP vectors were produced by $CaPO_4$-mediated transient co-transfection of the retroviral vector, *gag-pol*, and *env* encoding constructs at a ratio of 2.8:1.8:1 as described (66). All vector-containing supernatants were centrifuged, filtered, and concentrated by ultracentrifugation and resuspended in PBS, whereas producer cells were harvested to determine gag expression levels (see below). The physical titers were determined by monitoring the reverse transcriptase enzymatic activity of a certain volume of PBS-containing vectors as described (77). Infectious titer was determined by a single-round infectivity assay on *Fv1*-null MDTF cells. Virion infectivity was calculated by dividing the infectious titer by the physical titer.

Gag Expression and Processing—To test Gag expression, total proteins were extracted from producer cells in radioimmune precipitation assay buffer as described (66). Equal amounts of proteins were resolved on SDS-PAGE followed by immunoblot. Gag polyproteins were detected using a mouse

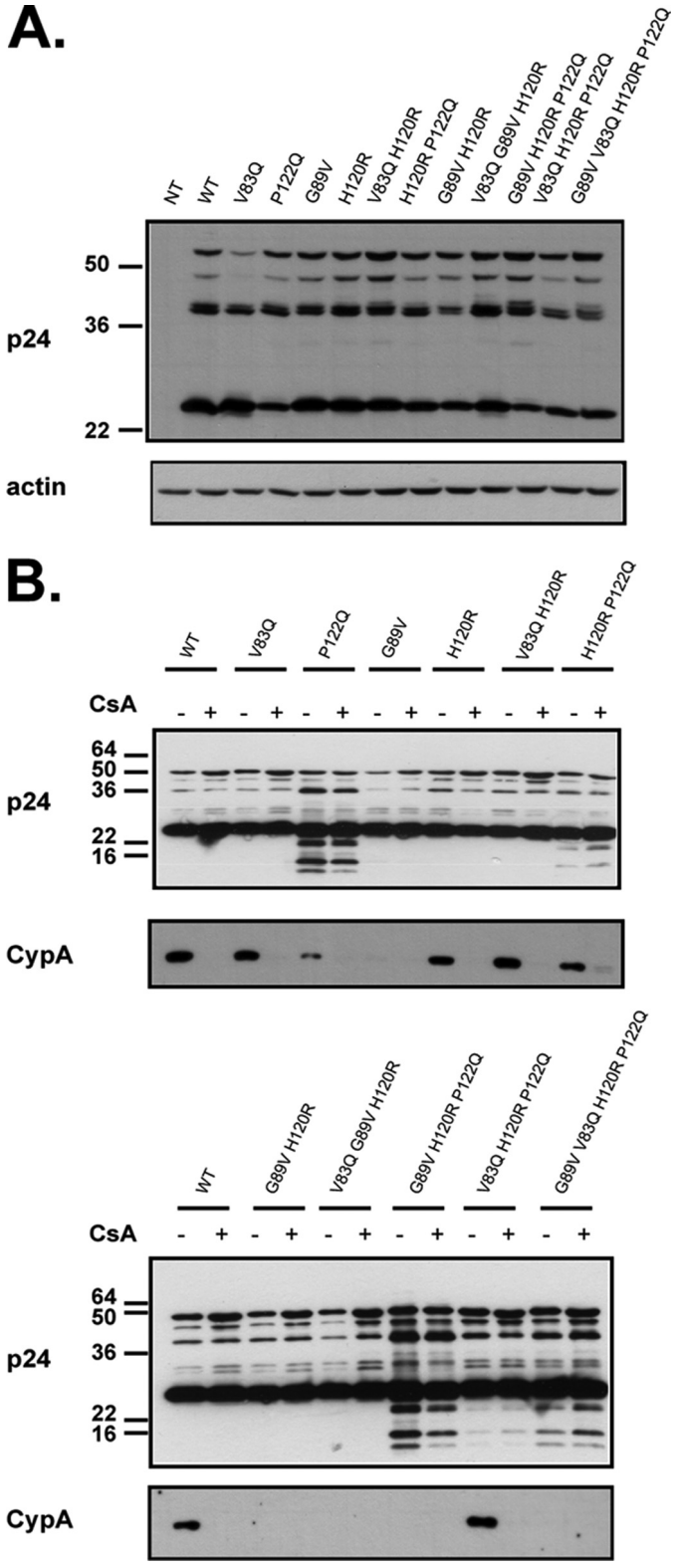

FIGURE 3. **Western blot analysis of HIV1 particles production.** *A*, shown is a Western blot of extracts from 293T cells transfected with the retroviral vector, the envelope plasmid, and the packaging construct harboring either a WT or a mutated CA and incubated with either anti-p24 (*top*)- or anti-actin (*bottom*)-specific antibodies. Of note, the structure of the HIV1 capsid used for the superimposition analysis (Fig. 2) displayed a leucine at CA83, yet the wild type HIV1-based vector used in this study harbored a valine at that position. *B*, shown are Western blots of concentrated virions harboring a CA with the indicated mutation produced in the presence (+) or absence (−) of CsA and analyzed using the anti-p24 (*top*) and anti-CypA antibodies.

TABLE 1

Physical and functional titers of HIV1 capsid mutants

The physical and functional titers were measured by the amount of reverse transcriptase activity in cpm/ml or the transducing units (TU) per ml, respectively. The relative infectivity was calculated by the ratio between the functional and physical titers. NI, non-infectious; ND, not done.

HIV1 strain	Physical titer	Functional titer	Relative infectivity	-Fold decrease in relative infectivity compared to WT
	10^8 cpm/ml	*10^8 TU/ml*	*TU/cpm*	
WT	8.0	7.6	0.95	1.0
V83Q	23.0	2.9	0.13	7.5
P122Q	5.5	NI	ND	ND
G89V	8.1	1.8	0.23	4.2
H120R	4.7	4.2	0.88	1.1
H120R/V83Q	8.1	1.6	0.20	4.7
H120R/P122Q	11.1	3.2	0.29	3.2
G89V/H120R	15.2	6.2	0.41	2.3
G89V/V83Q/H120R	12.9	4.0	0.31	3.0
G89V/H120R/P122Q	7.4	0.3	0.04	22.0
V83Q/H120R/P122Q	1.4	1.1	0.74	1.3
G89V/V83Q/H120R/P122Q	10.0	0.8	0.08	11.5

monoclonal antibody against the HIV1 capsid p24.[3] To ensure equal loading, the level of actin was assessed using a mouse monoclonal antibody (Chemicon) followed by a secondary sheep anti-mouse antibody conjugated to horseradish peroxidase (HRP). Viral proteins were analyzed by loading equal amounts of virions (based on reverse transcriptase activity as described (77)) on SDS-PAGE followed by immunoblot. Gag protein in virions was detected using the same antibody as described above. A polyclonal CypA-specific antibody followed by a donkey anti-rabbit HRP-conjugated antibody was used to determine CypA incorporation into virions.

Generation of Cell-stable Cell Lines—Retroviral vectors encoding TRIM5α variants were produced using the pLPCX-derived plasmids as described above. 5×10^4 MDTF were transduced with viral supernatants containing recombinant retroviral vectors and selected 3 days later by the addition of puromycin (Sigma) at a concentration of 5 μg/ml and maintained continuously in the presence of the drug. TRIM5α expression levels were determined by immunoblot as described (66). The HA-tagged proteins were detected using a peroxidase-conjugated rat monoclonal (clone 3F10, Roche Applied Science). Actin was used as a protein loading control and detected as described above.

Infection with GFP Reporter Vectors—MDTF cell lines were seeded at 2.5×10^4 in a 24-well plate and transduced 24 h later with, in the case of MLV-based vectors, 6 doses of 2-fold serial dilutions of GFP reporter vectors. Infections with HIV1-based GFP vectors were performed with 3 doses (in duplicate) or 6 doses of 2-fold serial dilutions starting with equal amounts of virions particles normalized by reverse transcriptase activity as described (77). In experiments using CsA, the drug was added at the time of infection at a concentration of 5 μM. Cells were harvested 3 days post-transduction, fixed in 1% formaldehyde-containing PBS, and resuspended in PBS 1% fetal calf serum. The percentage of GFP-positive cells was determined by flow cytometry using the BD Biosciences FACScan. Results were analyzed with FlowJo 8.1.1 software. The -fold restrictions were calculated as described (66).

[3] B. Chesebro and H. Chen, the AIDS Research and Reference Reagent Program.

RESULTS

Four Residues of the MLV Capsid Influence Restriction by Different Alleles of TRIM5α—Each orthologue of TRIM5α blocks a different range of retroviruses, yet the targeted capsids present a high degree of structural homology. We focused our attention on four MLV CA residues (CA82, CA109, CA110 and CA117) that were previously demonstrated to condition susceptibility to huTRIM5α, asking whether these positions also influenced MLV restriction by other TRIM5α species (19, 65, 66).

HuTRIM5α and rhTRIM5α both restrict N-MLV, albeit with different efficiencies, yet only the rhesus orthologue blocks HIV1 (16–19, 21, 78). However, huTRIM5α, with a change at arginine 332, gains the ability to restrict HIV1, at least to a certain extent (15, 79, 80). We, hence, engineered cell lines stably expressing a series of TRIM5α variants by retroviral vector-mediated transduction of permissive *Fv1*-null MDTF (Fig. 1*A*). We then challenged these cells with N- or B-MLV GFP vectors harboring either wild type capsid or a capsid mutated at one of the four critical positions and monitored infection by flow cytometry (Fig. 1*B*). Both wild type and R332A huTRIM5α could restrict N-MLV, as could rhTRIM5α, although to a lesser extent as expected. Single mutations at position 82 (Asn to Asp) or 117 (Leu to His) of the N-MLV capsid were sufficient to confer it with complete protection from rhTRIM5α, whereas combined mutations at these positions were required for the virus to significantly escape the block by R332A but not by wild type huTRIM5α (Fig. 1*B*). Conversely, although B-MLV was resistant to all three TRIM5α variants, replacing the CA glutamate 110 with an alanine was sufficient to render it susceptible to both huTRIM5α derivatives but not to rhTRIM5α, although we did find that the presence of an arginine at this position could render B-MLV more sensitive to the rhesus allele (Fig. 1*B*, supplemental Table S1). Additional changes at MLV CA82, CA109, CA110, and CA117 further indicated that these positions exert an influence on restriction by the three TRIM5α variants (supplemental Table S1).

Homology-based Identification of HIV1 Capsid Determinants Modulating huTRIM5α-mediated Restriction—The finding that some positions of the MLV capsid modulate re-

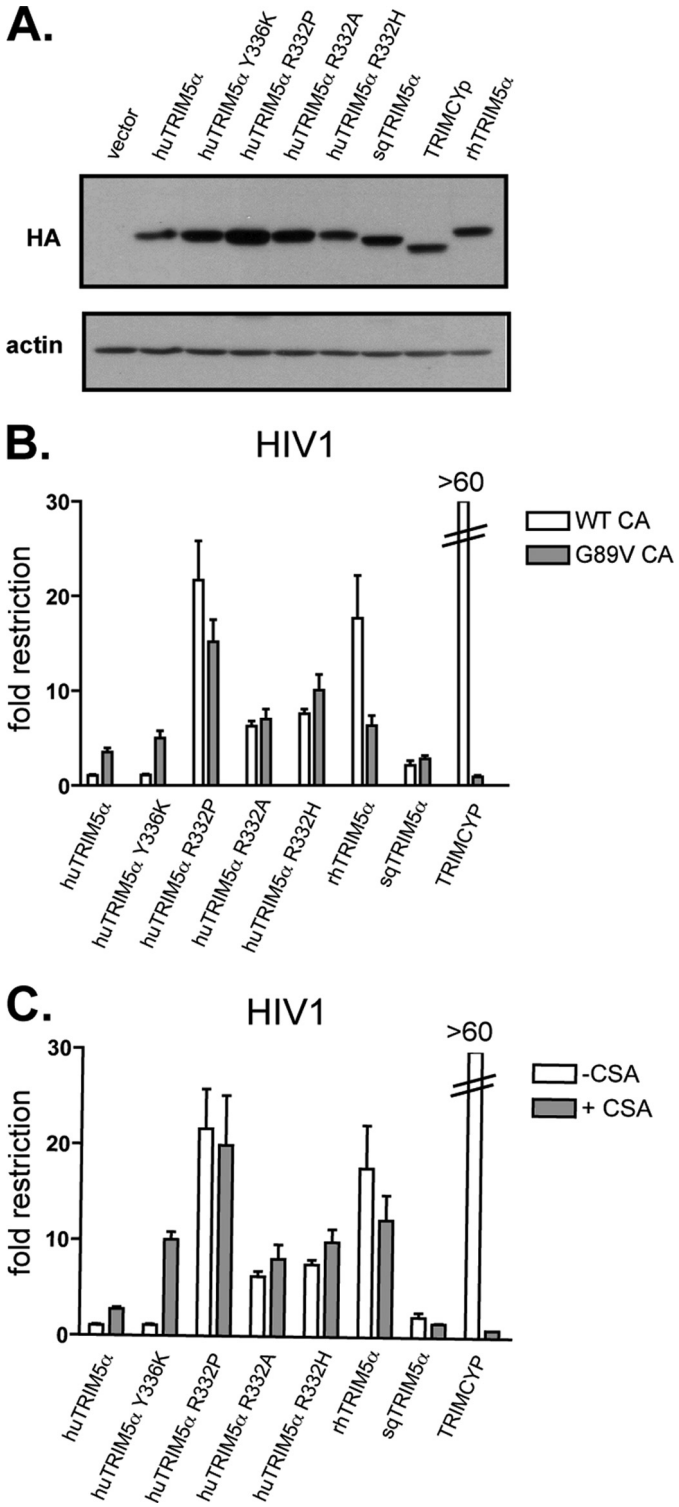

FIGURE 4. **Disruption of the CypA-CA interaction impacts differentially on restriction by distinct TRIM5α variants.** *A*, shown are expression levels of the various TRIM5 derivatives in stably transduced MDTF cell lines, documented at the time of viral challenge. Results are as originally observed (Fig. 1), indicating that expression of the transgenes was stable over time. *B*, MDTF cells expressing the indicated TRIM5α variant or transduced with a control vector (empty control) were challenged with serial 2-fold dilutions of HIV1 harboring a wild type (WT CA) or mutated (at CA89, termed G89V CA) capsid. Infections were scored at 72 h post-infection by FACS, and -fold restriction was calculated from the ratio of the percentage of GFP-positive cells between cells transduced with an empty vector and cells expressing a given variant of TRIM5α. Graphs shows the mean -fold restriction obtained with three different doses. *C*, the same is shown as in *B*, but cells were challenged with serial 2-fold dilutions of HIV1 harboring a wild type capsid in the presence (+*CsA*) or absence (−*CsA*) of the drug CsA. Of note, data shown in B and C were obtained from the same experiment displayed in two panels for clarity. These results are representative of two independent experiments.

striction of different TRIM5α variants suggests conservation in the modalities of TRIM5α-capsid recognition. However, HIV1 is protected from restriction by huTRIM5α, but not by huTRIM5α R332A and rhTRIM5α. Furthermore, a change at tyrosine 336 of huTRIM5α (huTRIM5α Y336K) was previously demonstrated to expand its activity toward B-MLV, Moloney MLV (Mo-MLV), SIVmac, and HIV-2, whereas HIV-1 and SIVagm were still able to escape restriction (66, 81). We, hence, sought to identify positions in the HIV1 capsid that were responsible for interfering with viral capture by both wild type and Y336K huTRIM5α.

We used the structural data available for the N-terminal domain of N- and B-MLV and HIV1 capsids to predict the three-dimensional structure of HIV2, SIVmac, and SIVagm capsids by assuming similar protein folding (27, 37, 38). We then performed a superimposition of these tertiary structures taking into account both primary sequences and structure alignments (Fig. 2*A*). Positions CA83, CA122, CA120, and CA129 on HIV-1 were found to be homologous to the four MLV capsid sites modulating TRIM5α-mediated restriction (Fig. 2, *B* and *C*). Interestingly, with the exception of CA129, residues found at these positions in HIV1 differ markedly from the amino acids present at homologous positions of other capsids (Fig. 2*C*). To test whether these identified HIV1 capsid positions interfere with restriction mediated by wild type or Y336K huTRIM5α, we substituted residues at HIV1 CA83 (V83Q), CA122 (P122Q), and CA120 (H120R) with the corresponding amino acids found on viruses restricted by either or both TRIM5α variants, *e.g.* N-, B-MLV, HIV2, and SIVmac (Fig. 2*C*). Because HIV1, in contrast to these latter viruses, binds the cellular protein CypA, we decided to include also a mutation of CA89 (G89V) that was previously demonstrated to disrupt this interaction (Fig. 2, *A* and *B*) (47–49).

Physical and Functional Characterization of HIV1 Capsid Mutants—We produced HIV1-based GFP vectors harboring single or combined mutations at positions CA83, CA89, CA122, and CA120. To investigate any effect of these mutations on Gag polyprotein expression, processing, and particle production, we analyzed Gag proteins in the producer cell as well as in the virions by immunoblot. No major change in steady-state Gag level was noted except for a slight reduction with the V83Q capsid mutation (Fig. 3*A*). Western blot analysis of purified virions revealed aberrant processing for most P122Q-containing capsids, (Fig. 3*B*), with corresponding decreases in viral infectivity (Table 1). However, combining the P122Q mutation with changes at CA83 and CA120 completely restored processing and infectivity (Table 1).

As the interaction between HIV1 capsid and CypA has been demonstrated to influence sensitivity to TRIM5α-mediated restriction, we also assessed the incorporation of CypA into all produced HIV-1 capsid mutants. For comparison,

TABLE 2
-Fold restriction of HIV-1 capsid mutants by various TRIM5α alleles

HIV strain	huTRIM5α derivatives					rhTRIM5α	sqTRIM5α	TRIMCyp
	WT	Y336K	R332P	R332A	R332H			
WT	1.1 ± 0.0	1.1 ± 0.0	11.1 ± 0.9	5.3 ± 0.3	6.1 ± 0.9	>20	1.3 ± 0.1	>20
V83Q	0.9 ± 0.1	1.1 ± 0.1	6.9 ± 0.8	3.7 ± 0.4	3.6 ± 0.2	>20	1.4 ± 0.1	>20
G89V	3.2 ± 0.1	3.8 ± 0.4	9.9 ± 1.0	4.8 ± 0.2	5.2 ± 0.2	7.9 ± 0.8	1.6 ± 0.0	1.4 ± 0.0
H120R	1.5 ± 0.2	3.0 ± 0.4	>20	10.0 ± 1.4	10.1 ± 2.5	>20	1.3 ± 0.1	>20
H120R/V83Q	1.2 ± 0.0	1.4 ± 0.0	>20	9.9 ± 1.3	9.2 ± 0.2	>20	1.4 ± 0.0	>20
H120R/ P122Q	4.3 ± 0.5	10.4 ± 1.2	>20	>20	>20	>20	1.2 ± 0.1	>20
G89V/ H120R	6.6 ± 1.3	8.1 ± 1.7	>20	11.5 ± 3.0	12.1 ± 4.0	17.5 ± 5.4	1.7 ± 0.3	1.5 ± 0.2
G89V/V83Q/H120R	5.6 ± 0.9	7.2 ± 1.5	>20	9.7 ± 1.8	12.4 ± 1.4	12.6 ± 2.7	1.4 ± 0.2	1.4 ± 0.1
G89V/H120R/P122Q	15.6 ± 3.7	16.1 ± 1.8	>20	19.1 ± 1.7	>20	17.0 ± 5.0	1.5 ± 0.1	1.3 ± 0.1
V83Q/ H120R/P122Q	2.0 ± 0.2	2.3 ± 0.2	>20	17.9 ± 2.8	13.2 ± 1.4	>20	1.3 ± 0.1	>20
G89V/V83Q/H120R/P122Q	10.3 ± 1.0	12.8 ± 1.6	>20	>20	19.2 ± 1.9	12.7 ± 2.2	1.3 ± 0.2	1.1 ± 0.1

each mutant was also produced in the presence of CsA, a drug that inhibits the capsid-CypA interaction. CypA could be detected in wild type HIV1 virions, whereas this incorporation was prevented by the presence of CsA during viral particle production or by an amino acid change at CA89 as expected. However, none of the single or combined mutations at positions CA83, CA120, and CA122 affected the incorporation of CypA into virions (Fig. 3*B*).

HIV1 CA83, CA89, CA120, and CA122 Modulate Sensitivity to huTRIM5α—We tested whether the identified HIV1 capsid positions could exert an influence on TRIM5α-mediated restriction as observed for their MLV counterparts. For this, we used our panel of viruses to challenge MDTF cells stably expressing various TRIM5α variants that had distinct activities against HIV1 and MLV (Figs. 1*A* and 4*A*). In addition to wild type huTRIM5α and rhTRIM5α, we included cells expressing the huTRIM5α Y336K mutant, which has an expanded restriction activity toward MLV strains yet remains inactive against HIV1 (66, 81). Conversely we generated cells expressing huTRIM5α with various changes at position 332 (R332P, R332A, R332H), all of which have been demonstrated to confer restriction activity against HIV-1, whereas their spectrum of MLV restriction is limited to N-MLV (15, 79, 80). Finally, two TRIM5α alleles from New World monkeys, neither of which blocks N-MLV, were included: owl monkey TRIMCyp, which inhibits HIV1 through a CA-CypA interaction, and squirrel monkey TRIM5α (sqTRIM5α), which has no effect on HIV1 (20, 60, 61, 82).

As expected, HIV1 could escape wild type and Y336K huTRIM5α as well as sqTRIM5α but was susceptible to all Arg-332 huTRIM5α mutants, to rhTRIM5α, and to TRIMCyp (Fig. 4*A*). Then, when a single point mutation was introduced at CA89 (G89V), HIV1 became partly susceptible to wild type and Y336K huTRIM5α (3–4-fold restriction, Fig. 4*A* and Table 2) but remained resistant to sqTRIM5α restriction. In contrast, this change in the HIV1 cyclophilin binding loop conferred either partial or complete protection toward rhTRIM5α and TRIMCyp restriction, respectively, as previously reported (54–56, 60, 61). Interestingly, the Arg-332 huTRIM5α mutants blocked wild type and CA G89V HIV1 with the same efficiency (Fig. 4*A*, Table 2). The same was observed with an HIV1 CA mutant (P90A) similarly reported not to bind CypA (data not shown) or when using the drug CsA, a known competitive inhibitor of the CypA-CA interaction (Fig. 4*B*). In the presence of CsA, HIV1 became more sensitive to wild type (3-fold) and Y336K huTRIM5α (10-fold) yet remained equally sensitive to Arg-332 mutants (Fig. 4*B*).

In the case of MLV, the canonical 110 position of the capsid plays a primary role as a determinant of huTRIM5α-mediated restriction (18, 66, 83). An arginine at the homologous position in HIV1, CA120, confers sensitivity to Y336K huTRIM5α but only has a slight effect on susceptibility to wild type huTRIM5α (Fig. 5 and Table 2). Further sensitivity toward both forms of TRIM5α was observed when a change at CA120 was combined with either a mutation at CA122 and/or at CA89, whereas protection against sqTRIM5α was maintained for all HIV1 capsid mutants (Fig. 5 and Table 2). These changes in HIV1 capsid led to a similar increase in restriction by rhTRIM5α and huTRIM5α Arg-332 mutants. In contrast, altering the amino acid at CA83 in the context of either a wild type or a mutated capsid allowed a slight escape of restriction from all TRIM5α variants (Table 2).

We then combined mutations at all four CA positions modulating HIV1 susceptibility to huTRIM5α (CA83, CA89, CA120, and CA122). The resulting HIV1 derivative was sensitive (around 10-fold restriction) to all three TRIM5α variants tested; that is, wild type, Y336K huTRIM5α, and rhTRIM5α (Fig. 5, Table 2).

As mentioned above, a change of amino acid at CA89 disrupts CypA binding, but alternatively, the mutation *per se* may increase the sensitivity of HIV1 to TRIM5α. We, therefore, tested, in the presence of CsA, single and combined mutations at CA83, CA120, and CA122 for their effect on TRIM5α susceptibility. CsA systematically increases the sensitivity of HIV1 mutants to both wild type and Y336K huTRIM5α (Fig. 5*B*). Yet, CsA treatment in some cases was less potent than the G89V mutation in increasing this susceptibility to TRIM5α, suggesting a CypA-independent contribution when a mutation is performed at CA89 (Fig. 5*B*).

Aromatic Residues Located within the Cavity Surrounded by Key Residues Are Essential for Gag Processing and HIV1 Infectivity—This study together with previous reports demonstrates that HIV1 and MLV escape TRIM5α restriction activity by a combination of residues located at the edge of a cavity (19, 66, 84). The positions of these amino acids at the surface of the capsid likely offer possibilities for viral escape by allowing mutations without altering capsid stability significantly. Yet TRIM5α may target residues located deeper within the cavity that are essential for virus infectivity. Their crucial role in capsid stability would mean that any mutations would not

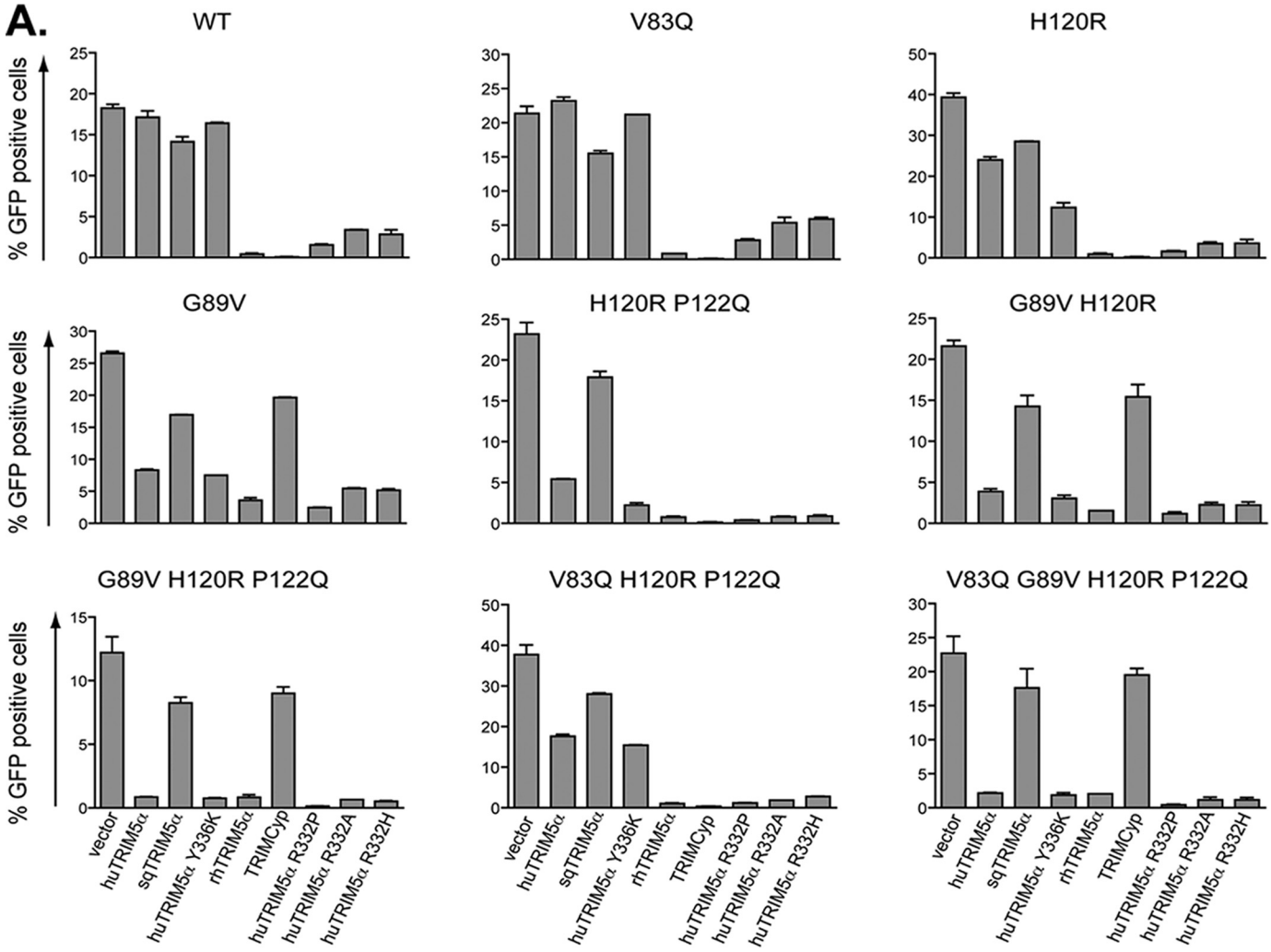

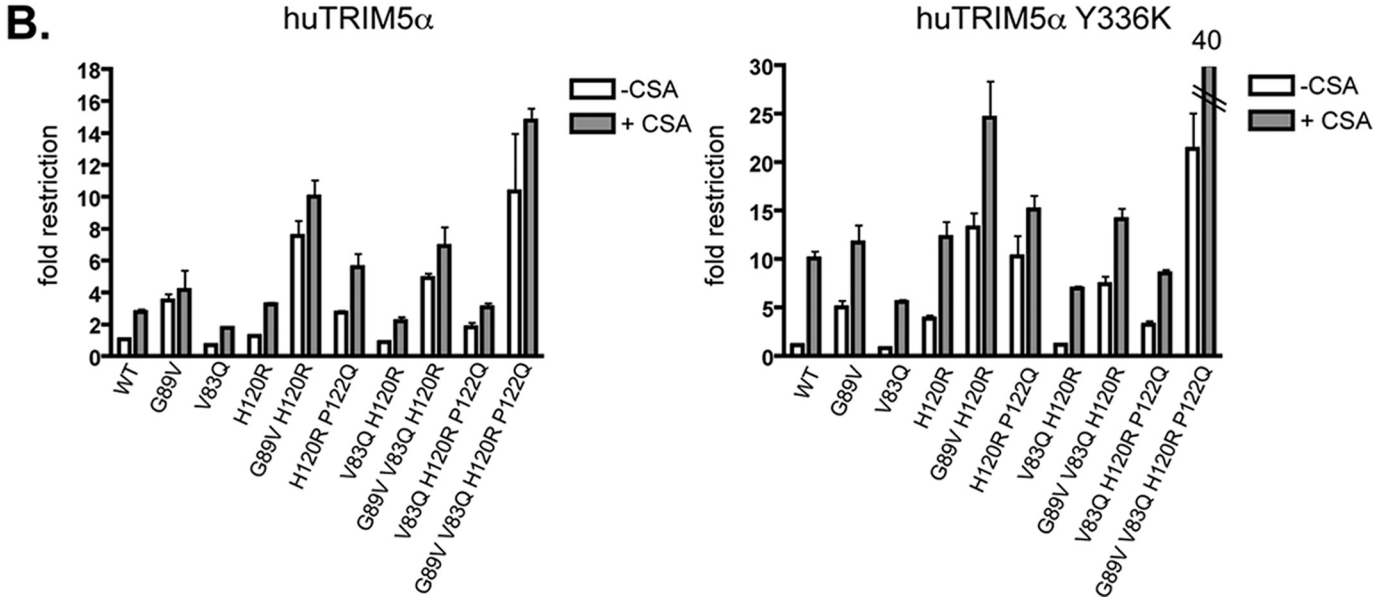

FIGURE 5. **HIV1 capsid positions CA83, CA89, CA120, and CA122 modulate TRIM5α restriction.** *A*, MDTF cells expressing the indicated TRIM5α variant or transduced with an empty vector were challenged with three different doses (in duplicate) of HIV1 vectors harboring either a WT or the indicated mutant CA. Infections were scored 72 h post-infection by flow cytometry. Graphs shows results obtained with a single dose, but similar results were observed with the two other doses. These results are representative of at least three independent experiments. *B*, MDTF expressing wild type (*left graph*) or Y336K huTRIM5α (*right graph*) were challenged with serial 2-fold dilutions of HIV-1 GFP vectors in the presence (+*CsA*) or absence of the drug cyclosporine A (−*CsA*). Scoring of the infections and calculation of the -fold restriction were performed as described in Fig. 4.

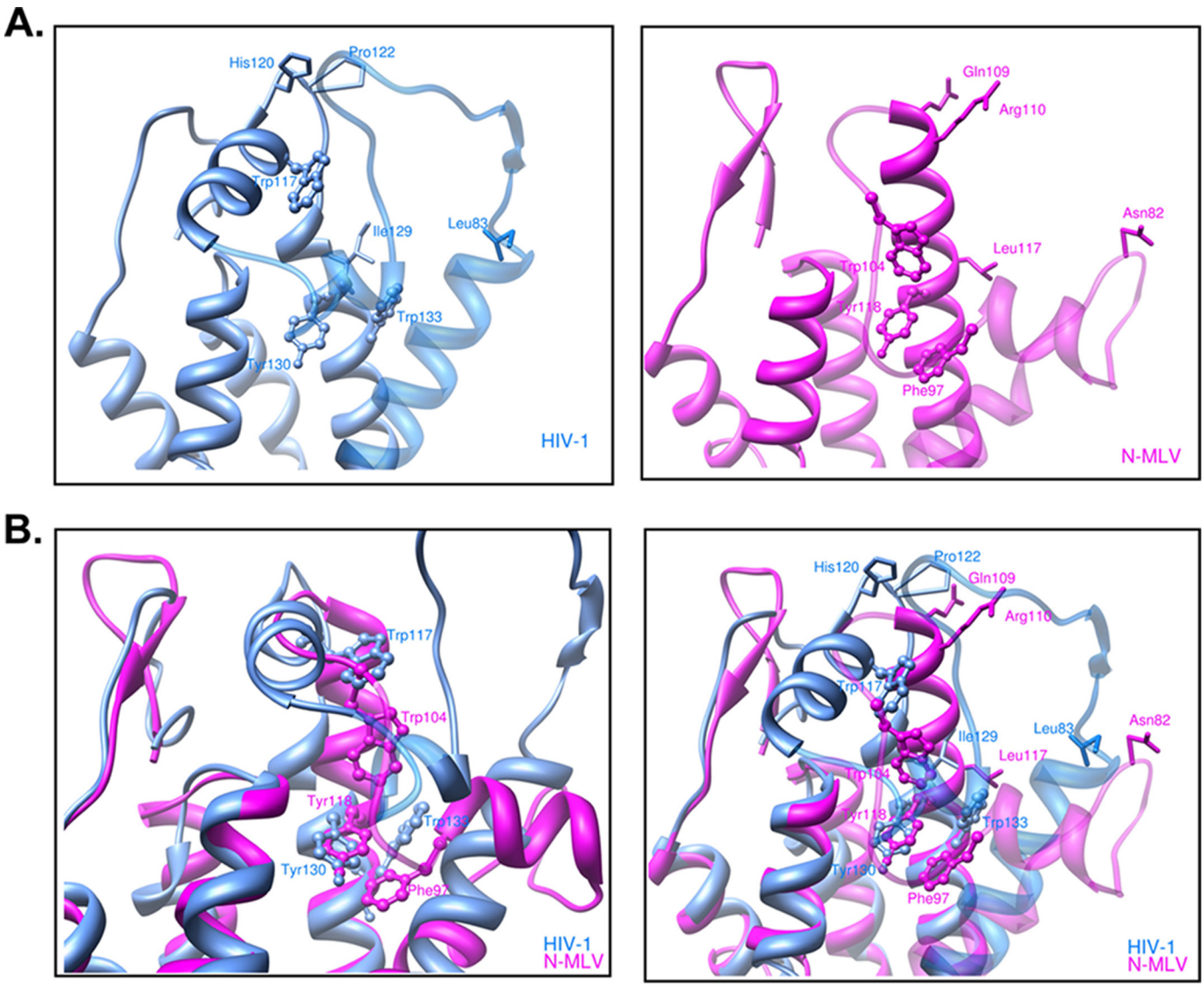
A.
His120
Pro122
Trp117
Ile129
Leu83
Trp133
Tyr130
HIV-1
Gln109
Arg110
Asn82
Leu117
Trp104
Tyr118
Phe97
N-MLV
B.
Trp117
Trp104
Tyr118
Trp133
Tyr130
Phe97
HIV-1
N-MLV
His120
Pro122
Gln109
Arg110
Trp117
Ile129
Leu83
Asn82
Leu117
Trp104
Tyr118
Trp133
Tyr130
Phe97
HIV-1
N-MLV
C.
Consensus
HIV1
HIV2
SIVAGM
SIVMAC
N-MLV
B-MLV

be tolerated by the virus, causing it to escape from TRIM5α by mounting obstacles in the way of this pocket through amino acid changes at the nearby positions CA83, CA89, CA120, CA122. Accordingly, three aromatic residues (phenylalanine 97, tryptophan 104, and tyrosine 118 in the MLV CA and tryptophan 133, tyrosine 130, and tryptophan 117 in the HIV1 CA) are located within this pocket and interact with each other (Fig. 6, *A* and *B*). These aromatic residues are conserved among the known and predicted structures of retroviral capsids that we analyzed (Fig. 6, *B* and *C*). To test their role in virus infectivity, we replaced these aromatic residues with alanine in both MLV and HIV1. All the resulting mutants were non-infectious in MDTF cells (Fig. 7*A*). Correlating this phenotype, Western blot analyses revealed particles with aberrantly processed Gag protein even though virion production itself was not dramatically altered (Fig. 7*B*).

DISCUSSION

TRIM5α-mediated retroviral restriction proceeds through direct binding of its PRYSPRY domain to the capsid of incoming viruses. Amino acids at four positions (CA82, CA109, CA110, and CA117) of the MLV capsid were previously demonstrated to shelter some MLV strains from huTRIM5α restriction (66). Here, we first demonstrate that several TRIM5α variants or orthologues (wild type and R332A huTRIM5α as well as rhTRIM5α), despite exhibiting different spectrums of anti-retroviral specificity, are all influenced in their action by the same four positions of the MLV capsid. In a second set of experiments, we demonstrate that structurally homologous positions on the HIV1 capsid similarly condition the recognition of this virus by the restriction factor. Together, these results attest to a high degree of conservation in the modalities of TRIM5α-CA recognition.

Comparing the influence of MLV CA82, CA109, CA110, and CA117 on huTRIM5α and rhTRIM5α restriction revealed that changes at several of these positions were required for the virus to escape the human version of the antiviral, whereas single changes were sufficient to decrease or suppress blockade by its rhesus counterpart. It is likely that these differences reflect selective pressures exerted by lineage-specific retroviral infections during the course of primate evolution, as does the inverse pattern of activities of human and rhesus TRIM5α on N-MLV and HIV1 (85). Along the same line, a single change at arginine 332 in huTRIM5α increases its ability to block HIV1, but we found that this is at the cost of a decreased activity against MLV. Consistent with this result, an amino acid substitution at that position was previously demonstrated to induce a loss of activity of huTRIM5α against an extinct *Gammaretrovirus* derived from *Pan troglodytes* endogenous retrovirus (PtERV) as well as toward B- and Mo-MLV (66, 86).

The present study also reveals striking similarities between the modes of recognition of both MLV and HIV1 capsids by TRIM5α. Capitalizing on our previous observation that amino acids at specific positions of the MLV capsid can interfere with TRIM5α-mediated blockade, we identified their structural homologues in the HIV capsid. Remarkably, we found that three of these HIV1 determinants (CA83, CA120, and CA122, corresponding to MLV CA82, CA110, and CA109, respectively) are major modulators of susceptibility to TRIM5α. Interestingly, HIV1 CA122 had previously been designated as homologous to MLV CA110 based on primary sequences alignment of both capsids, yet structural homology between them revealed that a small hinge at position 120 of HIV1 CA orients proline 122 of this protein similarly to glutamine 109 of the MLV capsid (87).

Replacing proline 122 of HIV1 CA by glutamine led to a loss of infectivity coincident with abnormal Gag processing. Interestingly, these defects could be suppressed by further mutating CA120. These data are consistent with an important role for these residues in ensuring normal capsid folding and as a consequence its proper subjection to cleavage by the viral protease during maturation, as suggested within the context of similar processing defects (88).

The CA H120R mutation increased HIV1 susceptibility more to Y336K huTRIM5α than to its huTRIM5α wild type counterpart. Combining mutations at both CA120 and CA122 further increased HIV1 sensitivity toward both huTRIM5α variants. These two positions lie in a loop linking helices 6 and 7 of CA, consistent with previous studies pointing to a role for this loop in determining susceptibility to TRIM5α-mediated restriction. Replacing this loop on SIVagm with the corresponding loop of HIV1 yields a virus with increased sensitivity to rhesus and African Green monkey TRIM5α (89). As well, specific positions within this domain (CA116 and CA119) were found to influence HIV1 replication in various primate cells, although their impact on sensitivity to the corresponding TRIM5α orthologues was not specifically tested (84). Furthermore, residues present in the homologous loops

FIGURE 6. **Three conserved aromatic residues at the bottom of a pit lined up by amino acids that are key modulators of TRIM5α restriction.** *A*, visualization of part of the previously defined secondary structure of the N-terminal domain of the HIV1 capsid (*top left panel*) and N-MLV capsid (*top right panel*) is shown. The aromatic residues Trp-133, Tyr-130, and Trp-117 are represented on the HIV1 capsid together with the four residues at positions 83, 120, 122, and 129. The structural homologues on the N-MLV counterpart are depicted with Phe- 97, Trp-104, and Tyr-1118 as well as the four residues at positions 82, 109, 110, and 117. Every amino acid is represented with its respective side chain *B*, shown is structure superimposition of both HIV-1 (*purple*) and N-MLV (*blue*) N-terminal domain of the capsid with the three structural homologous aromatic residues represented alone (*left panel*) or with the amino acids present at the four key positions (*right panel*). *C*, structural sequence alignments of HIV1, HIV2, SIVmac, SIVagm and N- and B-MLV capsid N-terminal domain based on a combination of residue identity/similarity and secondary structure correspondence (see "Experimental Procedures"). Residues located in α helices or β strands are framed with *yellow-* or *green-filled rectangles*, respectively. In the consensus sequence line, *red capital letters* correspond to residues that are identical in all sequences, whereas *magenta capital letters* correspond to residues that are highly conserved. In the sequence lines, colored residues correspond to highly conserved or even identical residues between sequences. These residues are colored according to their nature; *red* for positively charged residues, *magenta* for negatively charged residues, *green* for polar and neutral residues, *blue* for hydrophobic residues, and *orange* for glycine. The three aromatic residues that have similar positions after structure superimposition are highlighted; phenylalanine 97 in N-MLV with tryptophan 133 in HIV1 (*framed in violet*), tyrosine 118 in N-MLV with tyrosine 130 in HIV1 (*framed in red*), and tryptophan 104 in N-MLV with tryptophan 117 in HIV1 (*framed in black*).

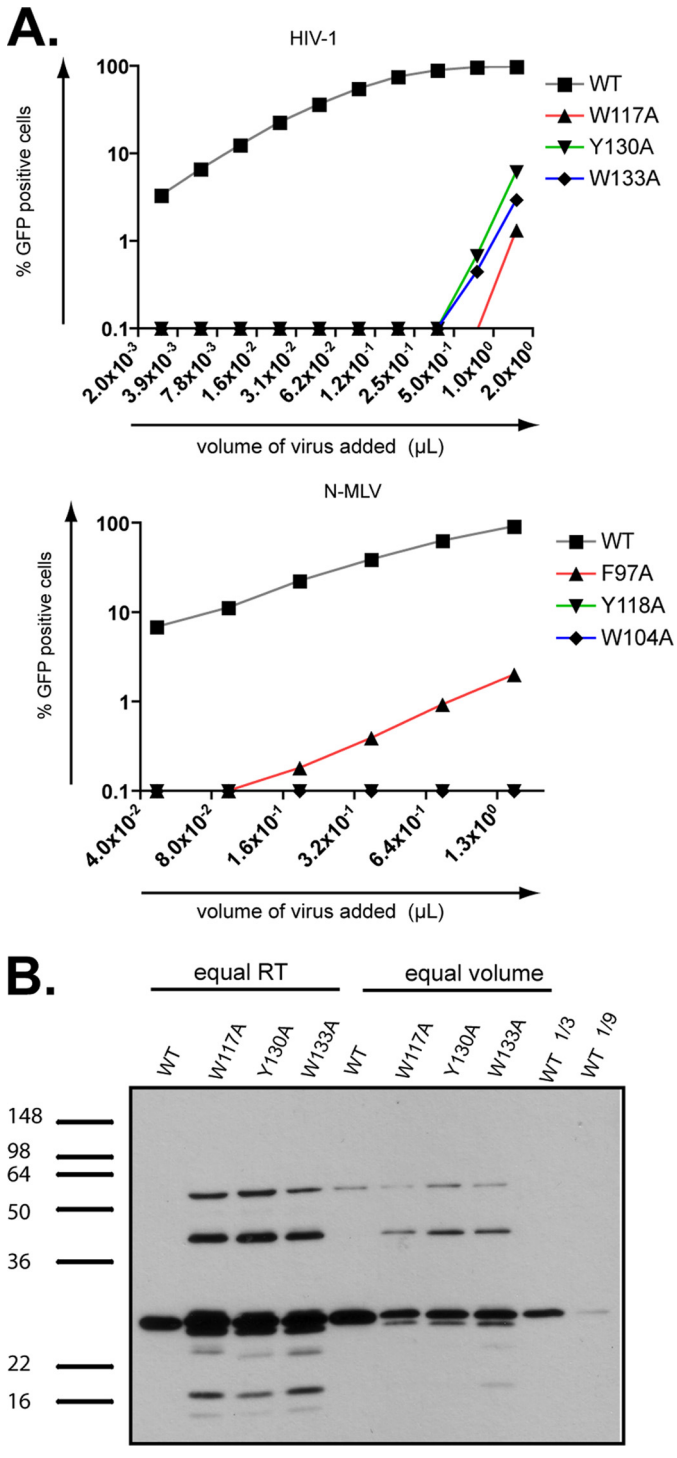

FIGURE 7. **Residues at the bottom of the putative TRIM5α recognition cavity are essential for proper Gag processing and viral infectivity.** *A*, HIV1 GFP vectors with a WT or mutant capsid at positions 117, 130, and 133 were analyzed by immunoblot using an anti-p24 specific antibody. Equal amounts of physical particles, normalized by measuring the reverse transcriptase activity (*equal RT*) or equal volumes of supernatant-containing vectors (*equal volume*) were loaded. For semiquantitative analysis, 3-fold (1/3) and 9-fold (1/9) dilutions of wild type HIV1 vectors were included. *B*, MDTF cells were challenged with serial 2-fold dilutions of HIV1 (*top graph*) or N-MLV (*bottom graph*) GFP vectors harboring either a WT or the indicated mutant capsid. Infectivity was scored 72 h later by FACS.

of other retroviral capsids were also shown to modulate susceptibility to TRIM5α; capsid positions 119 and 120 in SIVmac and HIV-2, respectively, affect the sensitivity to both human and cynomolgus monkey TRIM5α proteins (90).

In contrast to mutations at CA120 and CA122, substitution of valine 83 by glutamine reduced the susceptibility of several HIV1 capsid derivatives to TRIM5α-mediated restriction. As CA83 lies at the base of the CypA binding loop, it is tempting to speculate that it influences the orientation of this loop in a functionally relevant fashion.

Disruption of the CypA-CA interaction by the amino acid change G89V or by the use of the drug CsA augmented HIV1 sensitivity to both wild type and Y336K huTRIM5α. This is consistent with previous studies performed in cells overexpressing huTRIM5α and with the observation that virions with capsids deprived of their interaction with CypA but not wild type capsids can abrogate N-MLV restriction in human cells (52, 56, 87). This seems at odds with the finding that HIV1 sensitivity to disrupting CypA recruitment is independent of huTRIM5α (55, 57). TRIM5α overexpression, thus, appears to allow the detection of differential effects not apparent at physiological levels. Interestingly, CsA treatment had a greater impact on HIV susceptibility to Y336K huTRIM5α (10-fold) than to wild type huTRIM5α (3-fold). It has previously been demonstrated that Y336K mutation expands the spectrum of antiretroviral activity of huTRIM5α toward B-, Mo-MLV, HIV2, and SIVmac (66, 81). In contrast, HIV1 and SIVagm fully escape this block, whereas FIV is only partially restricted (81). Interestingly, HIV1, SIV, and FIV are the only retroviruses whose capsids have been described to bind CypA (41, 47, 49, 51, 52). The mutation Y336K may induce a conformational change such that huTRIM5α docking with the capsid is now more sensitive to the presence of CypA.

When arginine 332 of huTRIM5α was replaced by proline, alanine, or histidine, CypA recruitment by the HIV1 capsid lost its protective effect, as illustrated by the HIV CA G89V mutant or infections performed in the presence of CsA. No structural data are available yet for the TRIM5α PRYSPRY domain, but extrapolating from the crystal structure of related proteins, it is predicted that position 332 of TRIM5α lies in an exposed loop that constitutes the so-called variable region 1 (91–93). Therefore, a mutation at arginine332 may modify the conformation of the variable region 1 (such that TRIM5α alleviates the interference caused by CypA binding and/or catalytic activity, which ultimately improves capsid recognition). Interestingly, consistent with a high degree of conservation in the modalities of TRIM5α-CA recognition, sqTRIM5α, which is inactive against N-MLV, did not exert significant restriction activity against an HIV1 derivative where critical positions of the capsid were substituted by their N-MLV homologues. Yet sqTRIM5α-mediated restriction of SIVmac was shown to be dependent on residues located in the region homologous to the CypA binding loop of HIV1 (20). Therefore, further modifications of the HIV1 capsid may render it susceptible to this restriction factor. Reciprocally, mutating specific residues of the PRYSPRY or coiled-coil domains of sqTRIM5α may con-

fer it with the ability to block N-MLV as well as wild type or mutant HIV1 (94).

The CA83, CA120, and CA122 positions modulate restriction by TRIM5α, and the structurally homologous positions in MLV (CA82, CA109, and CA110) were previously demonstrated to influence sensitivity not only to TRIM5α but also to the mouse restriction factor Fv1. It seems unlikely that mutating these residues has global effects on CA structure, which would indirectly affect distantly located restriction factor binding sites. Rather, we favor a model in which the virus uses residues at these key positions to shelter the TRIM5α and Fv1 target sites, which themselves cannot be mutated without loss of capsid function. HIV1 CA83, -120, and -122 and MLV CA82, -109, and -110 are indeed situated on the edges of a pit, at the bottom of which reside three aromatic residues (phenylalanine 97, tryptophan 104, tyrosine 118 in the MLV CA and tryptophan 133, tyrosine 130, and tryptophan 117 in the HIV1 CA) that cannot be mutated without inducing aberrant Gag processing and loss of viral infectivity. These residues or others deeply situated in the pit might represent the TRIM5α recognition site, and viral escape is, thus, accordingly achieved by mounting obstacles to TRIM5α penetration into this pocket through changes at the more lenient yet critically placed CA82, CA109, CA110, and CA117 for MLV and, for HIV1, CA83, CA120, and CA122 acting in concert with the overhanging CypA binding loop. As such, resistance to TRIM5α is reminiscent of escape from neutralizing antibodies by glycosylation of the viral envelope, where sugar moieties hide critical protein epitopes (95, 96). Whether this apparent Achilles' heel in the HIV1 capsid can be targeted by antiviral therapies warrants investigation.

Acknowledgments—We thank Greg Towers for the pCXCR-sqTRIM5α plasmid, Priscilla Turelli for advice, Helen Rowe for reading the manuscript, and Sujana Nylakonda and Charlène Raclot for technical assistance. The modeling part of this work was performed within the Protein Modeling Facility of the University of Lausanne. Molecular graphics images were produced using the UCSF Chimera package from the Resource for Biocomputing, Visualization, and Informatics at the University of California, San Francisco (supported by National Institutes of Health Grant P41 RR-01081).

REFERENCES

1. Bieniasz, P. D. (2004) *Nat. Immunol.* **5,** 1109–1115
2. Wolf, D., and Goff, S. P. (2008) *Annu. Rev. Genet.* **42,** 143–163
3. Huthoff, H., and Towers, G. J. (2008) *Trends Microbiol.* **16,** 612–619
4. Sokolskaja, E., and Luban, J. (2006) *Curr. Opin. Microbiol.* **9,** 404–408
5. Towers, G. J. (2007) *Retrovirology* **4,** 40
6. Nisole, S., Stoye, J. P., and Saïb, A. (2005) *Nat. Rev. Microbiol.* **3,** 799–808
7. Ozato, K., Shin, D. M., Chang, T. H., and Morse, H. C., 3rd. (2008) *Nat. Rev. Immunol.* **8,** 849–860
8. Kar, A. K., Diaz-Griffero, F., Li, Y., Li, X., and Sodroski, J. (2008) *J. Virol.* **82,** 11669–11681
9. Langelier, C. R., Sandrin, V., Eckert, D. M., Christensen, D. E., Chandrasekaran, V., Alam, S. L., Aiken, C., Olsen, J. C., Kar, A. K., Sodroski, J. G., and Sundquist, W. I. (2008) *J. Virol.* **82,** 11682–11694
10. Perez-Caballero, D., Hatziioannou, T., Yang, A., Cowan, S., and Bieniasz, P. D. (2005) *J. Virol.* **79,** 8969–8978
11. Rhodes, D. A., de Bono, B., and Trowsdale, J. (2005) *Immunology* **116,** 411–417
12. Stremlau, M., Perron, M., Lee, M., Li, Y., Song, B., Javanbakht, H., Diaz-Griffero, F., Anderson, D. J., Sundquist, W. I., and Sodroski, J. (2006) *Proc. Natl. Acad. Sci. U.S.A.* **103,** 5514–5519
13. Ohkura, S., Yap, M. W., Sheldon, T., and Stoye, J. P. (2006) *J. Virol.* **80,** 8554–8565
14. Song, B., Gold, B., O'Huigin, C., Javanbakht, H., Li, X., Stremlau, M., Winkler, C., Dean, M., and Sodroski, J. (2005) *J. Virol.* **79,** 6111–6121
15. Stremlau, M., Perron, M., Welikala, S., and Sodroski, J. (2005) *J. Virol.* **79,** 3139–3145
16. Hatziioannou, T., Perez-Caballero, D., Yang, A., Cowan, S., and Bieniasz, P. D. (2004) *Proc. Natl. Acad. Sci. U.S.A.* **101,** 10774–10779
17. Keckesova, Z., Ylinen, L. M., and Towers, G. J. (2004) *Proc. Natl. Acad. Sci. U.S.A.* **101,** 10780–10785
18. Perron, M. J., Stremlau, M., Song, B., Ulm, W., Mulligan, R. C., and Sodroski, J. (2004) *Proc. Natl. Acad. Sci. U.S.A.* **101,** 11827–11832
19. Yap, M. W., Nisole, S., Lynch, C., and Stoye, J. P. (2004) *Proc. Natl. Acad. Sci. U.S.A.* **101,** 10786–10791
20. Ylinen, L. M., Keckesova, Z., Wilson, S. J., Ranasinghe, S., and Towers, G. J. (2005) *J. Virol.* **79,** 11580–11587
21. Stremlau, M., Owens, C. M., Perron, M. J., Kiessling, M., Autissier, P., and Sodroski, J. (2004) *Nature* **427,** 848–853
22. Wilson, S. J., Webb, B. L., Maplanka, C., Newman, R. M., Verschoor, E. J., Heeney, J. L., and Towers, G. J. (2008) *J. Virol.* **82,** 7243–7247
23. Ganser-Pornillos, B. K., Yeager, M., and Sundquist, W. I. (2008) *Curr. Opin. Struct. Biol.* **18,** 203–217
24. Byeon, I. J., Meng, X., Jung, J., Zhao, G., Yang, R., Ahn, J., Shi, J., Concel, J., Aiken, C., Zhang, P., and Gronenborn, A. M. (2009) *Cell* **139,** 780–790
25. Ganser-Pornillos, B. K., Cheng, A., and Yeager, M. (2007) *Cell* **131,** 70–79
26. Li, S., Hill, C. P., Sundquist, W. I., and Finch, J. T. (2000) *Nature* **407,** 409–413
27. Mortuza, G. B., Haire, L. F., Stevens, A., Smerdon, S. J., Stoye, J. P., and Taylor, I. A. (2004) *Nature* **431,** 481–485
28. Pornillos, O., Ganser-Pornillos, B. K., Kelly, B. N., Hua, Y., Whitby, F. G., Stout, C. D., Sundquist, W. I., Hill, C. P., and Yeager, M. (2009) *Cell* **137,** 1282–1292
29. Berthet-Colominas, C., Monaco, S., Novelli, A., Sibaï, G., Mallet, F., and Cusack, S. (1999) *EMBO J.* **18,** 1124–1136
30. Campos-Olivas, R., Newman, J. L., and Summers, M. F. (2000) *J. Mol. Biol.* **296,** 633–649
31. Cornilescu, C. C., Bouamr, F., Yao, X., Carter, C., and Tjandra, N. (2001) *J. Mol. Biol.* **306,** 783–797
32. Gamble, T. R., Vajdos, F. F., Yoo, S., Worthylake, D. K., Houseweart, M., Sundquist, W. I., and Hill, C. P. (1996) *Cell* **87,** 1285–1294
33. Gitti, R. K., Lee, B. M., Walker, J., Summers, M. F., Yoo, S., and Sundquist, W. I. (1996) *Science* **273,** 231–235
34. Jin, Z., Jin, L., Peterson, D. L., and Lawson, C. L. (1999) *J. Mol. Biol.* **286,** 83–93
35. Khorasanizadeh, S., Campos-Olivas, R., and Summers, M. F. (1999) *J. Mol. Biol.* **291,** 491–505
36. Kingston, R. L., Fitzon-Ostendorp, T., Eisenmesser, E. Z., Schatz, G. W., Vogt, V. M., Post, C. B., and Rossmann, M. G. (2000) *Structure* **8,** 617–628
37. Momany, C., Kovari, L. C., Prongay, A. J., Keller, W., Gitti, R. K., Lee, B. M., Gorbalenya, A. E., Tong, L., McClure, J., Ehrlich, L. S., Summers, M. F., Carter, C., and Rossmann, M. G. (1996) *Nat. Struct. Biol.* **3,** 763–770
38. Mortuza, G. B., Dodding, M. P., Goldstone, D. C., Haire, L. F., Stoye, J. P., and Taylor, I. A. (2008) *J. Mol. Biol.* **376,** 1493–1508
39. Braaten, D., Aberham, C., Franke, E. K., Yin, L., Phares, W., and Luban, J. (1996) *J. Virol.* **70,** 5170–5176
40. Bukovsky, A. A., Weimann, A., Accola, M. A., and Göttlinger, H. G. (1997) *Proc. Natl. Acad. Sci. U.S.A.* **94,** 10943–10948
41. Lin, T. Y., and Emerman, M. (2006) *Retrovirology* **3,** 70
42. Bosco, D. A., Eisenmesser, E. Z., Pochapsky, S., Sundquist, W. I., and

Kern, D. (2002) *Proc. Natl. Acad. Sci. U.S.A.* **99,** 5247–5252
43. Bosco, D. A., and Kern, D. (2004) *Biochemistry* **43,** 6110–6119
44. Braaten, D., Franke, E. K., and Luban, J. (1996) *J. Virol.* **70,** 3551–3560
45. Howard, B. R., Vajdos, F. F., Li, S., Sundquist, W. I., and Hill, C. P. (2003) *Nat. Struct. Biol.* **10,** 475–481
46. Li, Y., Kar, A. K., and Sodroski, J. (2009) *J. Virol.* **83,** 10951–10962
47. Franke, E. K., Yuan, H. E., and Luban, J. (1994) *Nature* **372,** 359–362
48. Luban, J., Bossolt, K. L., Franke, E. K., Kalpana, G. V., and Goff, S. P. (1993) *Cell* **73,** 1067–1078
49. Thali, M., Bukovsky, A., Kondo, E., Rosenwirth, B., Walsh, C. T., Sodroski, J., and Göttlinger, H. G. (1994) *Nature* **372,** 363–365
50. Braaten, D., Franke, E. K., and Luban, J. (1996) *J. Virol.* **70,** 4220–4227
51. Diaz-Griffero, F., Vandegraaff, N., Li, Y., McGee-Estrada, K., Stremlau, M., Welikala, S., Si, Z., Engelman, A., and Sodroski, J. (2006) *Virology* **351,** 404–419
52. Zhang, F., Hatziioannou, T., Perez-Caballero, D., Derse, D., and Bieniasz, P. D. (2006) *Virology* **353,** 396–409
53. Hatziioannou, T., Perez-Caballero, D., Cowan, S., and Bieniasz, P. D. (2005) *J. Virol.* **79,** 176–183
54. Berthoux, L., Sebastian, S., Sokolskaja, E., and Luban, J. (2005) *Proc. Natl. Acad. Sci. U.S.A.* **102,** 14849–14853
55. Keckesova, Z., Ylinen, L. M., and Towers, G. J. (2006) *J. Virol.* **80,** 4683–4690
56. Stremlau, M., Song, B., Javanbakht, H., Perron, M., and Sodroski, J. (2006) *Virology* **351,** 112–120
57. Sokolskaja, E., Berthoux, L., and Luban, J. (2006) *J. Virol.* **80,** 2855–2862
58. Brennan, G., Kozyrev, Y., and Hu, S. L. (2008) *Proc. Natl. Acad. Sci. U.S.A.* **105,** 3569–3574
59. Newman, R. M., Hall, L., Kirmaier, A., Pozzi, L. A., Pery, E., Farzan, M., O'Neil, S. P., and Johnson, W. (2008) *PLoS Pathog.* **4,** e1000003
60. Nisole, S., Lynch, C., Stoye, J. P., and Yap, M. W. (2004) *Proc. Natl. Acad. Sci. U.S.A.* **101,** 13324–13328
61. Sayah, D. M., Sokolskaja, E., Berthoux, L., and Luban, J. (2004) *Nature* **430,** 569–573
62. Virgen, C. A., Kratovac, Z., Bieniasz, P. D., and Hatziioannou, T. (2008) *Proc. Natl. Acad. Sci. U.S.A.* **105,** 3563–3568
63. Wilson, S. J., Webb, B. L., Ylinen, L. M., Verschoor, E., Heeney, J. L., and Towers, G. J. (2008) *Proc. Natl. Acad. Sci. U.S.A.* **105,** 3557–3562
64. Price, A. J., Marzetta, F., Lammers, M., Ylinen, L. M., Schaller, T., Wilson, S. J., Towers, G. J., and James, L. C. (2009) *Nat. Struct. Mol. Biol.* **16,** 1036–1042
65. Lassaux, A., Sitbon, M., and Battini, J. L. (2005) *J. Virol.* **79,** 6560–6564
66. Maillard, P. V., Reynard, S., Serhan, F., Turelli, P., and Trono, D. (2007) *PLoS Pathog.* **3,** e200
67. Wu, C. H., Apweiler, R., Bairoch, A., Natale, D. A., Barker, W. C., Boeckmann, B., Ferro, S., Gasteiger, E., Huang, H., Lopez, R., Magrane, M., Martin, M. J., Mazumder, R., O'Donovan, C., Redaschi, N., and Suzek, B. (2006) *Nucleic Acids Res.* **34,** D187–D191
68. Berman, H. M., Westbrook, J., Feng, Z., Gilliland, G., Bhat, T. N., Weissig, H., Shindyalov, I. N., and Bourne, P. E. (2000) *Nucleic Acids Res.* **28,** 235–242
69. Edgar, R. C. (2004) *BMC Bioinformatics* **5,** 113
70. Edgar, R. C. (2004) *Nucleic Acids Res.* **32,** 1792–1797
71. Jern, P., Sperber, G. O., and Blomberg, J. (2005) *Retrovirology* **2,** 50
72. Sali, A., and Blundell, T. L. (1993) *J. Mol. Biol.* **234,** 779–815
73. Pettersen, E. F., Goddard, T. D., Huang, C. C., Couch, G. S., Greenblatt, D. M., Meng, E. C., and Ferrin, T. E. (2004) *J. Comput. Chem.* **25,** 1605–1612
74. Needleman, S. B., and Wunsch, C. D. (1970) *J. Mol. Biol.* **48,** 443–453
75. Henikoff, S., and Henikoff, J. G. (1992) *Proc. Natl. Acad. Sci. U.S.A.* **89,** 10915–10919
76. Kabsch, W., and Sander, C. (1983) *Biopolymers* **22,** 2577–2637
77. Aiken, C., and Trono, D. (1995) *J. Virol.* **69,** 5048–5056
78. Perron, M. J., Stremlau, M., and Sodroski, J. (2006) *J. Virol.* **80,** 5631–5636
79. Li, Y., Li, X., Stremlau, M., Lee, M., and Sodroski, J. (2006) *J. Virol.* **80,** 6738–6744
80. Yap, M. W., Nisole, S., and Stoye, J. P. (2005) *Curr. Biol.* **15,** 73–78
81. Diaz-Griffero, F., Perron, M., McGee-Estrada, K., Hanna, R., Maillard, P. V., Trono, D., and Sodroski, J. (2008) *Virology* **378,** 233–242
82. Song, B., Javanbakht, H., Perron, M., Park, D. H., Stremlau, M., and Sodroski, J. (2005) *J. Virol.* **79,** 3930–3937
83. Towers, G., Bock, M., Martin, S., Takeuchi, Y., Stoye, J. P., and Danos, O. (2000) *Proc. Natl. Acad. Sci. U.S.A.* **97,** 12295–12299
84. Hatziioannou, T., Cowan, S., Von Schwedler, U. K., Sundquist, W. I., and Bieniasz, P. D. (2004) *J. Virol.* **78,** 6005–6012
85. Goldschmidt, V., Ciuffi, A., Ortiz, M., Brawand, D., Muñoz, M., Kaessmann, H., and Telenti, A. (2008) *J. Virol.* **82,** 2089–2096
86. Kaiser, S. M., Malik, H. S., and Emerman, M. (2007) *Science* **316,** 1756–1758
87. Towers, G. J., Hatziioannou, T., Cowan, S., Goff, S. P., Luban, J., and Bieniasz, P. D. (2003) *Nat. Med.* **9,** 1138–1143
88. von Schwedler, U. K., Stemmler, T. L., Klishko, V. Y., Li, S., Albertine, K. H., Davis, D. R., and Sundquist, W. I. (1998) *EMBO J.* **17,** 1555–1568
89. Lin, T. Y., and Emerman, M. (2008) *Virology* **379,** 335–341
90. Song, H., Nakayama, E. E., Yokoyama, M., Sato, H., Levy, J. A., and Shioda, T. (2007) *J. Virol.* **81,** 7280–7285
91. Grütter, C., Briand, C., Capitani, G., Mittl, P. R., Papin, S., Tschopp, J., and Grütter, M. G. (2006) *FEBS Lett.* **580,** 99–106
92. James, L. C., Keeble, A. H., Khan, Z., Rhodes, D. A., and Trowsdale, J. (2007) *Proc. Natl. Acad. Sci. U.S.A.* **104,** 6200–6205
93. Woo, J. S., Imm, J. H., Min, C. K., Kim, K. J., Cha, S. S., and Oh, B. H. (2006) *EMBO J.* **25,** 1353–1363
94. Maillard, P. V., Ecco, G., Ortiz, M., and Trono, D. (2010) *J. Virol.* **84,** 5790–5801
95. Pantophlet, R., Wang, M., Aguilar-Sino, R. O., and Burton, D. R. (2009) *J. Virol.* **83,** 1649–1659
96. Raska, M., Takahashi, K., Czernekova, L., Zachova, K., Hall, S., Moldoveanu, Z., Elliott, M. C., Wilson, L., Brown, R., Jancova, D., Barnes, S., Vrbkova, J., Tomana, M., Smith, P. D., Mestecky, J., Renfrow, M. B., and Novak, J. (2010) *J. Biol. Chem.* **285,** 20860–20869